2021 43rd Annual International Conference of the
IEEE Engineering in Medicine & Biology Society (EMBC)
Oct 31 - Nov 4, 2021. Virtual Conference

Different brain functional networks between subjective cognitive decline and health control based on graph theory

Zhuoyuan Li, Ying Han, and Jiehui Jiang*, *Member, IEEE*

***Abstract*—Subjective cognitive decline (SCD) is a preclinical stage before cognitive impairment, which has a high conversion risk into Alzheimer's disease. However, it is still unknown on the brain functional differences between SCD and healthy controls (HC) subjects. This study therefore proposed a complex brain network analysis based on graph theory. In this study, we selected functional magnetic resonance imaging (fMRI) scans from Xuanwu Hospital of Capital Medical University, including 27 SCD and 42 HC subjects. First, we constructed brain functional connectivity network to obtain brain network topology parameters, including clustering parameters, shortest path length, global efficiency, local efficiency, small world attributes, and modularity. Then, we compared differences on the parameters between two groups. As a result, both SCD and HC groups showed the characteristics of small world. Both global efficiency and local efficiency of HC groups were higher than those of the SCD group. In addition, we found that the global modularity of the SCD group (6 modules) was higher than the HC group (7 modules). Our findings indicated that there were differences in brain functional networks between SCD and HC groups. Graph theory analysis may be useful and helpful to discriminate SCD and HC subjects.**

***Keywords*—subjective cognitive decline (SCD), Alzheimer's disease (AD), functional magnetic resonance imaging (fMRI), graph theory, modularity**

I. Introduction

Alzheimer's disease (AD) is one of the most common progressive neurodegenerative diseases, which causes irreversible damage to the memory and other cognitive functions of the elderly in modern society. Currently, there is no effective drug treatment [1]. Subjective cognitive decline (SCD) is the preclinical stage of AD [2]. Although there is no evidence of AD like pathological features in the pathogenesis of SCD, more and more studies support the correlation between SCD and AD characteristics. Therefore, SCD has been widely considered as a high-risk stage before cognitive impairment [3].

In recent years, the development of various imaging technologies makes it possible to analyze brain functional networks for AD [1]. As a frequently used functional imaging, functional magnetic resonance imaging (fMRI) based on blood oxygen level dependence (BOLD) has been widely used in AD research [4]. In addition, the complex brain network analysis based on graph theory has been widely used in AD, which provides a new perspective for AD diagnosis [5]. However, it is still unknown on the brain functional differences between SCD and healthy controls (HC) subjects.

Therefore, this study constructed and compared the brain functional network of the SCD and HC groups, trying to determine the differences of brain function between the two groups, and seek the imaging sensitivity characteristics of SCD, so as to provide an important basis for SCD research. The outcomes of this study may provide new insights into the pathogenesis of AD in the preclinical stage.

II. Materials and Methods

A. Participants, imaging scanning and preprocessing

The experimental data used in this study were all recruited from the memory clinic of the Neurology Department of Xuanwu Hospital, Beijing, China. The inclusion criteria of SCD is as follows [6]: (1) self-reported memory has continued to decline compared to the previous (within 5 years); (2) Mini-Mental State Examination (MMSE) and Montreal Cognitive Assessment (MCA) scores are within normal ranges; (3) non-clinical depression (GDS score < 6). In addition, the SCD subjects would be excluded if subjects exist severe depression, stroke, cognitive decline caused by disease, history of psychosis or traumatic brain injury. All the HC subjects were right-handed people of Han nationality and had no history of cognitive impairment or other related mental diseases. Finally, this study included 69 participants. Among them, 27 were SCD and the rest were HC. Clinical characteristics including age, sex, education, Mini-mental state examination (MMSE), Montreal cognitive assessment-B (MoCa-B) and Global deterioration scale (GDS) were collected and listed in Table 1. As a result, there was no difference between the two groups in clinical characteristics.

TABLE I. The clinical data of two cohorts

	HC(n=42)	*SCD(n=27)*	*P value*
Age	66.2±4.2	65.6±4.5	0.575[b]
Education	12.9±2.9	12.4±2.7	0.520[b]
Male/Female	19:23	7:20	0.106[a]
MMSE	28.9±1.2	28.8±2.0	0.830[b]
MoCA-B	26.1±1.9	26.6±2.0	0.299[b]
GDS	2.2±3.1	2.7±2.3	0.499[b]

Values are presented as the mean ± standard deviation (SD).

a the p value was obtained by $\chi 2$ test, b the p value was obtained by two-sample t tests

All SCD and HC subjects were scanned with 3.0T superconducting MR and 12 channel phased array coils.

*Research supported by the National Natural Science Foundation of China No.61603236, 61633018.

Zhuoyuan Li, Jiehui Jiang are with the Shanghai Institute for Advanced Communication and Data Science, Shanghai University, Shanghai, China (corresponding author to provide phone: +86 139-1892-0926; e-mail: jiangjiehui@shu.edu.cn).

Ying Han is with Center of Alzheimer's Disease, Institute for Brain Disorders, Beijing, China.

Gradient echo plane pulse sequence was used to collect resting state fMRI data. The scanning range covered all brain tissues from skull base to skull top. Scanning parameters (nearly 7 min) were as following: repetition time (TR) / echo time (TE) = 2000 / 30 ms, 3.5 mm slice thickness, 0.7 mm slice spacing, 224 × 224 field of view, 64 × 64 matrix, 90 ° rotation angle, 240 time points were collected, scanning time was 6 min and 40 s.

The preprocessing of fMRI data was carried out using the Data Processing Assistant for Resting-state fMRI (DPASF; http://www.rfmri. org/DPARSF). The first 10 time points fMRI images were discarded to achieve magnetization balance. The rest of the time-point images were initially corrected. The corrected images were aligned with the average image of all images with respect to time for head movement correction. Then, we positioned the functional image on the structural images for registration. Finally, all images were normalized to Montreal Neurological Institute (MNI) standard space with a 3mm ×3mm ×3mm spatial resolution, and were spatially smoothed (8 mm FWHM of Gaussian kernel), linearly DE trended and temporally filtered (0.01-0.08 Hz). The amplitude of low frequency fluctuations (ALFF) maps and fractional amplitude of low frequency fluctuations (f/ALFF) maps were then calculated and normalized by the global mean and standard deviation of ALFF values within a whole brain mask.

B. Brain Network Construction

In this study, we constructed 90 brain network matrices to analyze the topological characteristics of brain functional network. The first step was to define the nodes of the brain network. We selected the Standardized Automated Anatomical Labeling (AAL) template (90 regions of interest) as the mask to extract brain regions as nodes. The average voxel value of each node was calculated and normalized, and the average voxel was used as the node value. Secondly, an interrelated correlation matrix was calculated based on partial correlation coefficients, while eliminating the influence of covariance such as age, gender and education. Finally, after obtaining the correlation coefficient matrix, the sparse threshold method was used to determine whether there was a connection between each two nodes. The correlation coefficient matrix was then transformed into a binary matrix set with different sparsity thresholds. In this study, in order to ensure that there were no isolated nodes in the brain network under the full sparsity threshold, we used 0.09 as the start of sparsity. We set 0.01 as the interval and 0.5 as the end of the sparsity.

C. Brain Network Analysis

In order to describe the topologic organization of the brain network, the following parameters were calculated: clustering coefficient (C), shortest path length (L), local efficiency (localE), global efficiency (globalE), and small-world parameters including gamma, lambda and sigma. The clustering coefficient C represents the degree of aggregation of nodes in the network graph. The shortest path length reflects the speed of information transmission between two nodes. The shorter the length of the shortest path is, the faster the information transmission rate is. The local efficiency and global efficiency indicate the efficiency of exchanging information in the whole network or local network respectively. The small world parameters show the metrics of the network. The small world network satisfies when the gamma and sigma values are much greater than 1, and the lambda value is equal to 1.

We also calculate the modularity of each network. The module is defined as a set of relatively sparse connections with the nodes in the external module, while the nodes in the internal module are highly interconnected. This concept was first proposed by Newman and Girvan in 2004 [7]. It has been widely used as a result of the division of quantitative modules. In this study, we applied the grey optimization method proposed by Clauset to calculate modularity [8]. The formula is as follows:

$$\mathrm{M} = \sum_{S=1}^{N_M} \left[\frac{l_S}{L} - \left(\frac{d_S}{2L} \right)^2 \right] \quad (1)$$

where N_M means the number of modules, L is the total number of edges in the whole network, l_S is the total number of edges connecting two nodes in module S, and d_S is the total degree of all nodes in module S. It is generally considered that the maximum value of network modularity m > 0.3 indicates that the network has the modular structure.

D. Statistical analysis

Demographic characteristics were compared between SCD and HC groups using two-sample t test or the chi-square t test. The comparison of the brain network parameters under the same sparsity between the two groups were all using the two-sample t test. All statistical analyses were performed in SPSS Version 22.0 software (SPSS Inc., Chicago, IL). All P value < 0.05 was considered significant differences.

III. RESULTS

A. Construction of brain network

Figure 1 showed the partial correlation matrix. In the partial correlation matrix, the color corresponds to the correlation coefficient. The axis represented 90 brain regions in AAL template.

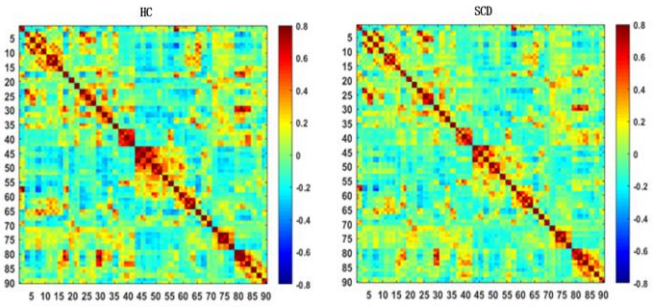

Figure 1. The partial correlation coefficient matrixes of the SCD and HC groups.

B. Network parameters

Fig 2 showed the results of network parameters including C, L, localE, globalE, gamma, lambda and sigma under 9% to 50% sparsity in two groups.

Compared with HC group, SCD group has lower cluster coefficient under all sparsity settings. The clustering coefficients of the two groups increased with the increase of

sparsity threshold. As for the shortest path length L, the values of the SCD group and the HC group are very close. Both global efficiency and local efficiency of HC group were higher than those of SCD group, and increased with the increase of sparsity threshold. However, the local efficiency of SCD is significantly higher than that of HC. Both HC and SCD groups showed that gamma >> 1, lambda ≈ 1 and sigma >> 1 in all sparse matrices.

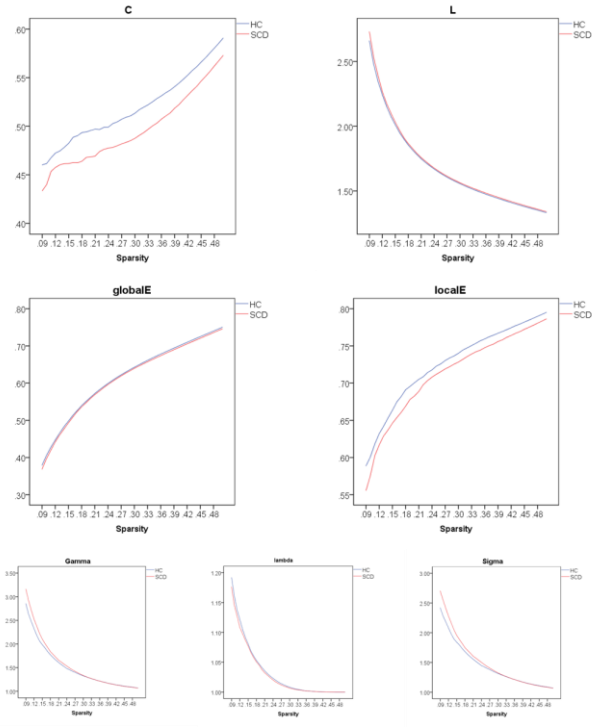

Figure 2. Network parameters including C, L, globalE, localE, Gamma, Lambda, Sigma. The abscissa is sparsity from 9% to 50%. The blue curve represents HC group and the red curve represents SCD group.

C. Modularity and module structure

Figure 3 showed the trend of global modularization in two brain networks with 9-50% sparsity. We found that when the modularity was greater than 0.3, the sparsity threshold was less than 20%, and both SCD and HC groups had modularity. The modularity of brain network decreased with the increase of sparsity threshold. When the sparsity threshold was 10%, the modularity of the SCD group was 0.52, while that of the HC group was 0.51.

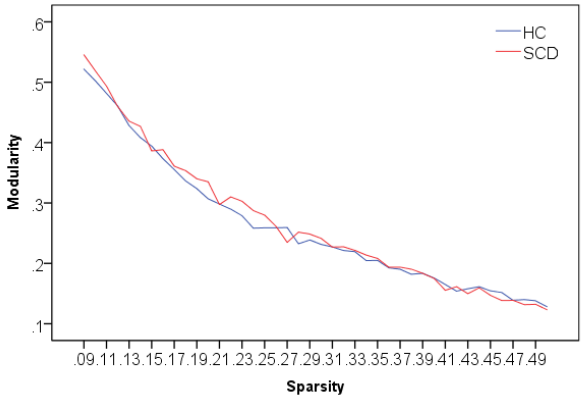

Figure 3. Modularity of the HC and SCD groups.

Figure 4 shows a visualized brain network diagram with a sparsity threshold of 9% (minimal value to guarantee full connection of network). The seven modules of HC were recorded as Module H1-H7. Module H1 included anterior central gyrus, middle frontal gyrus, inferior insular gyrus, inferior triangular gyrus and central sulcus tectum; module H2 included dorsolateral superior frontal gyrus, medial superior frontal gyrus, orbital superior frontal gyrus and rectus gyrus; module H3 included orbital inferior frontal gyrus, insula, hippocampus, anterior cingulate gyrus and para cingulate gyri, amygdala and para hippocampal gyrus; module H4 included cortex, cuneiform lobe and occipital cortex around talus fissure Module H5 included thalamus, caudate nucleus and lenticular nucleus, pallidum; module H6 included medial and para cingulate gyrus, superior parietal gyrus, inferior parietal angular gyrus and superior marginal gyrus; module H7 includes inferior temporal gyrus, middle temporal gyrus and temporal pole.

The brain network of SCD group was divided into six modules, which were recorded as module P1-P6. Module P1 included orbital superior frontal gyrus, orbital middle frontal gyrus, rectus gyrus and caudate nucleus; module P2 included insular inferior frontal gyrus, trigonal inferior frontal gyrus, posterior cingulate gyrus and angular gyrus; module P3 included inferior occipital gyrus, fusiform gyrus, cuneiform lobe and lingual gyrus; module P4 included supplementary motor area, anterior central gyrus, dorsolateral superior frontal gyrus; module P5 included thalamus, caudate nucleus, lenticular nucleus, pallidum; module P6 included thalamus It includes superior, middle and inferior temporal gyrus, temporal pole, hippocampus, para hippocampal gyrus and amygdala.

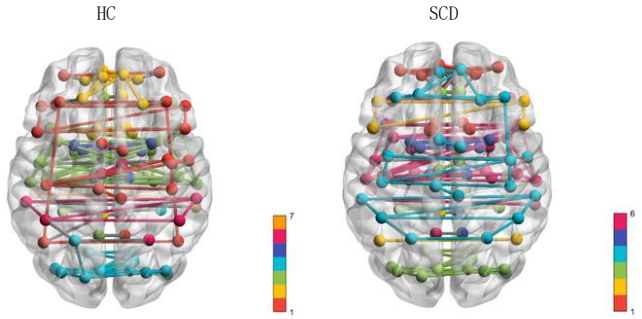

Figure 4. Visualized brain connectivity of HC and SCD groups (left is HC, right is SCD).

IV. Discussion

A. Between-group comparisons

A large number of studies have shown that human brain functional networks had small world properties, while networks with neurological diseases have been transferred from random networks into conventional networks [9]. In this study, both SCD and HC groups showed small world properties. We found that when the sparsity increases, the sigma of both the SCD group and the HC group will decrease and become close. This result meant that the brain network of SCD group was similar to that of HC group. Therefore, graph

theory analysis showed that SCD was not a neurological disease, which was consistent with previous studies.

In this study, the clustering coefficient of SCD group was significantly lower than that of HC group. Clustering coefficient represented the connection efficiency between nodes and surrounding nodes, which meant that SCD group has the ability of local integration and information processing [10]. As for the shortest path length, SCD group was still slightly higher than HC group. The shortest path length represented the rate of information transfer between nodes [11]. The ability to transmit information between nodes decreased in SCD group compare to HC group.

In addition, both the global efficiency and the local efficiency of HC group were higher than those of SCD group. Some studies also found that the overall efficiency of AD group in the whole brain was significantly reduced [12]. Our study was consistent with previous research.

B. Modularity and module structure

Using module analysis, we reflected the properties and functional connections of brain network. The results of this study showed that the number of brain network modules in the SCD group is reduced, which is consistent with previous studies [13]. As shown in Figure 4, we observed that the connection of the SCD group in the frontal lobe was lost, which was related to memory loss. In addition, the connection of the angular gyrus in the SCD group was also lost, which was related to visual and auditory functions. Therefore, when the connection is poor, it will cause a series of obstacles. This is also consistent with previous research [14].

C. Limitations

Although differences could be observed between SCD and HC using brain network analysis, there were some limitations that need to be considered. First of all, there were not many data samples, which meant that the experimental results cannot fully represent all SCD subjects. Secondly, AAL template with 90 regions was used in this study. The brain template used was symmetrical, but actually individual human brain had various shapes. So it would lead to some differences in biased results. Thirdly, the partial correlation matrix was used to calculate the network parameters. This might lead to biased results. We planned to use other correlation matrix to see the differences in the future.

V. CONCLUSION

In this work, we used graph theory method to analyze the differences of brain functional networks between SCD and HC groups. The results showed that both groups showed the properties of small world, while the SCD group showed the enhancement of small world characteristics. Both groups showed modularity, and the modularity of SCD group was enhanced. Our findings indicate that the brain function network between SCD and HC subjects has changed. In addition, graph theory analysis may be useful and helpful to discriminate SCD and HC subjects.

REFERENCES

[1] Yan T Y, Wang W H, Yang L, et al. Rich club disturbances of the human connectome from subjective cognitive decline to Alzheimer's disease[J]. Theranostics, 2018, 8(12): 3237-3255.

[2] Molinuevo J L, Rabin L A, Amariglio R, et al.Implementation of subjective cognitive decline criteria in research studies[J]. Alzheimer & Dementia, 2017, 13(3): 296-311.

[3] Lopez-Sanz D, Garces P, Alvarez B, el al. Network disruption in the preclinical stages of Alzheimer's disease: from subjective cognitive decline to mild cognitive impairment[J]. Int. J. Neural Syst, 2017, 27(8).

[4] Gratton C, Laumann T O, Nielsen AN, et al. Functional Brain Networks Are Dominated by Stable Group and Individual Factors, Not Cognitive or Daily Variation[J]. Neuron, 2018, 98(2): 439.

[5] Martensson G, Pereira J B, Mecocci P, et al. Stability of graph theoretical measures in structural brain networks in Alzheimer's disease[J]. Sci. Rep, 2018, 8.

[6] Vannini P, Hanseeuw B, Munro C E, et al.Hippocampal hypometabolism in older adults with memory complaints and increased amyloid burden[J]. Neurology, 2017, 88(18): 1759-1767.

[7] Girvan M, Newman M E J. Community structure in social and biological networks[J]. Proceedings of the National Academy of Sciences of the United States of America, 2002, 99(12): 7821-7826.

[8] Clauset A, Newman M E J, Moore C.Finding community structure in very large networks[J]. Phys. Rev. E, 2004, 70(6).

[9] Duan H Q, Jiang J H, Xu J, et al. Differences in A beta brain networks in Alzheimer's disease and healthy controls[J]. Brain Res, 2017, 1655: 77-89.

[10] Dai Z J, Lin Q X, Li T, et al. Disrupted structural and functional brain networks in Alzheimer's disease[J]. Neurobiology of Aging, 2019, 75: 71-82.

[11] Lo C Y, Wang P N, Chou K H, et al. Diffusion Tensor Tractography Reveals Abnormal Topological Organization in Structural Cortical Networks in Alzheimer's Disease[J]. J. Neurosci, 2010, 30(50): 16876-16885.

[12] Afshari S, Jalili M. Directed Functional Networks in Alzheimer's Disease: Disruption of Global and Local Connectivity Measures[J]. IEEE J Biomed Health Inform, 2017, 21(4): 949-955.

[13] He Y, Chen Z, Evans A. Structural insights into aberrant topological patterns of large-scale cortical networks in Alzheimer's disease[J]. J. Neurosci, 2008, 28(18): 4756-4766.

[14] Onoda K, Yamaguchi S. Small-worldness and modularity of the resting-state functional brain network decrease with aging[J]. Neurosci. Lett, 2013, 556(556): 104-108.